ANS MC2015 - Joint International Conference on Mathematics and Computation (M&C), Supercomputing in Nuclear Applications (SNA) and the Monte Carlo (MC) Method · Nashville, Tennessee · April 19–23, 2015, on CD-ROM, American Nuclear Society, LaGrange Park, IL (2015)

PROTON-INDUCED GAIN IN A PORTABLE FARADAY CUP

Shaun Marshall and Blake Currier
Department of Physics
Worcester Polytechnic Institute
100 Institute Rd, Worcester, MA 01609

Andrew D Hodgdon, CHP
Radsim, LLC
584 Grove St, Newton, MA 02462
adhodgdon@radsim.org

ABSTRACT

A Portable Faraday Cup (PFC) is being designed to calibrate therapy-range proton accelerators (50 to 250 MeV). The PFC must be accurate to 1% and practical, hence vacuum-less and of low mass. Copper was chosen as the detector core, coated with a Kapton insulating film and silver ground. The Monte Carlo method (MCNP6 and Geant4) was used to simulate the radiation cascade and predict gain versus height (H), diameter (D) and insulator thickness (K). H and D were mostly functions of proton range; both are proportional to mass and inversely so to proton leakage, and thus decreases detector accuracy. Kapton functions to capture backscattered electrons, the function of the fields in a standard Faraday Cup. Greater K increases capture but increases secondary electron in-leakage. Determining optimal K was made difficult by the lack of low energy proton and electron cross-sections. A secondary electron model was programmed with the SDEF command for the MCNP model based on recently published cross-section approximations. This secondary electron source method was benchmarked against a series of experimental measurements of protons on copper and on water.

Key Words: Monte Carlo, Geant4, MCNP6, Faraday Cup

1 INTRODUCTION

In modern radiation therapy, protons have become an increasingly popular method of treating cancer near critical structures, with many dosimetric advantages of charged particle interactions (CITE). A novel, portable, vacuumless Faraday Cup for detecting charged particles was designed to calibrate proton therapy facilities, in energies ranging from 50 to 250 MeV. The detector is constructed of a copper cylinder, coated with Kapton insulation and grounded with silver (CITE). Monte Carlo computational simulations in MCNP6 (CITE) and GEANT4 (CITE) were performed to evaluate radiation cascade effects and predict signal versus height, diameter and insulator thickness characteristics.

Preliminary results indicated that increasing the mass of the Faraday Cup's conductor reduced proton leakage but increased the system accuracy. While additional Kapton captures more primary and secondary electrons, it also increases secondary electron leakage into the copper. Optimizing

this Kapton thickness has been made difficult by the lack of low energy proton and electron cross-sections in current Monte Carlo based simulation programs (CITE). A comprehensive secondary electron evaluation of the Kapton was performed and benchmarked against a series of experimental measurements by J. Gordon et al. [1]

In corroboration with the computational calculations, three prototype Faraday Cup devices were constructed by Pyramid Technical Consultants, Inc. (Waltham, Ma), each having a different thickness of Kapton. The units were tested in Germany to determine accuracy of the new design.

2 EXPERIMENTAL BACKGROUND

2.1 Go99

2.2 HIT Beam Stop Calibration

3 SIMULATION RESULTS

3.1 MCNP6

MCNP version 6.1 with standard cross-section libraries was used to simulate gain. The Faraday Cup geometry is shown in Fig. 1. The height of the cylinder is fixed at 10 cm. The diameter is varied from 2 to 10 cm and the Kapton thickness is varied from 25 to 75 microns. The materials are standard copper, Kapton, silver and air at STP. The source is a 2 cm diameter proton beam at 250 MeV. This is the maximum expected energy. A suitable diameter for this energy will be suitable for lower energies. Physics was turned on for seven particles: neutrons, photons, electrons, protons, deuterons, tritons and alphas.

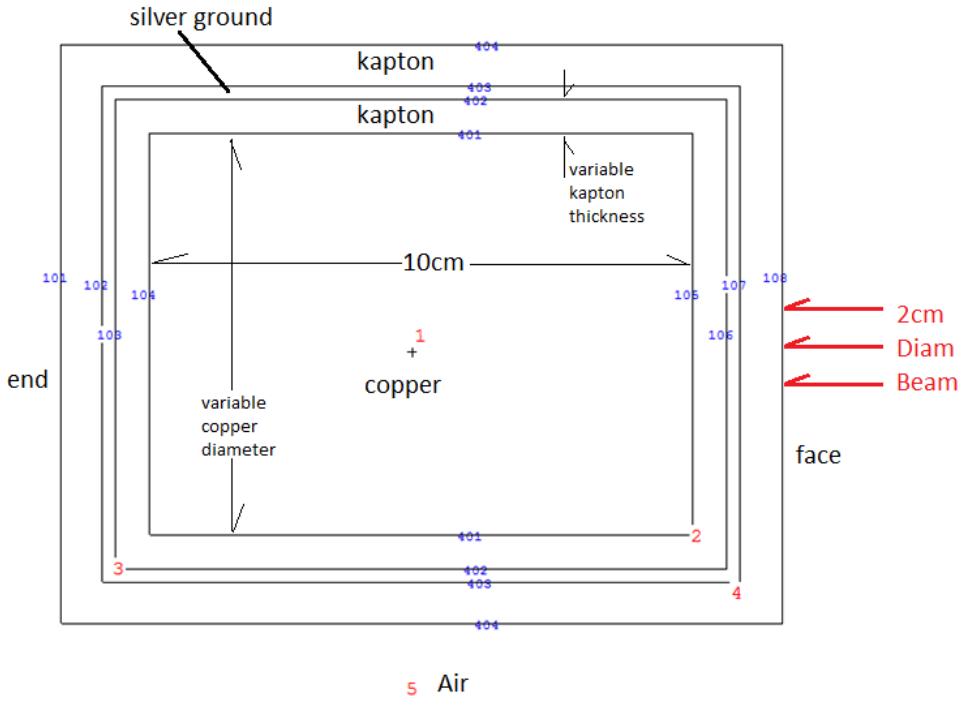

Figure 1. Geometry from side of horizontal copper cylinder

Gain was modeled simplistically by tallies of two charged particles (protons and electrons) crossing three surfaces (face, side and end). Gain is expressed in terms of elemental charge deposited in copper per beam proton, shown in eq. 1.

$$Gain = \frac{\sum Q_{particle \rightarrow Cu} - \sum Q_{particle \leftarrow Cu}}{\sum Q_{P+\ beam}} \tag{1}$$

MCNP6 distinguishes between two types of secondary electrons, those that are created by proton collisions, i.e., SE_h, (MCNP cannot track such electrons) and those that are generated by other particles (notably photons that are themselves secondary), i.e., $SE_{!h}$. It was assumed that for the selection of a good copper diameter the SE_h are not important. This assumption was not tested.

It is assumed that protons and electrons are the only contributors to gain. This was tested (for $SE_{!h}$ only) and found to be true within a factor of 2E-4.

It was also assumed that the detailed behavior of $SE_{!h}$ electrons in Kapton (i.e., capture causing mirror charge in copper) has little effect on the choice of copper diameter. This means that the location and energy of electrons captured in the kapton do not have to be tallied to get a good answer for the copper diameter; this assumption was not tested.

The detector is to be a beam proton counter. The perfect detector will yield a gain of unity, i.e.,

1 exactly, seen in eq. 2

$$Error = (Gain - 1) \cdot 100\% \tag{2}$$

3.2 Geant4

Geant4 is an object-oriented C++ toolkit for developing applications which simulate the passage of particles through matter. Libraries of cross-section tables, elemental/molecular properties, and pre-defined stochastic physics processes allow for rapid, intuitive invocation of necessary system setup commands. Once initialized, “Manager" modules cooperate to organize and accumulate dynamic information which is organized in the following chronology:

1. The **DetectorConstruction** class is called to verify, store and lock the predefined geometry.
2. The **G4UIManager** initializes upon successful compilation and execution of the *main()* routine. If a visualizer is selected, **G4VisManager** is also invoked.
3. The user issues the command to execute a macro file of *runs*; each run is characterized by the defined beam particle type, the beam energy, and the number of *events*, or number of such isolated simulations. If multithreading is available, **G4RunManager** allocates the events to the available worker threads on a rolling basis.
4. For each event, the simulation of the *primary* (beam) particle proceeds, constructing a new *track*, or well-defined trajectory for every particle not at rest.
5. The behavior of every track is determined dynamically, with each *step*, or stochastically occuring physical process (collisions, absorbtions, etc) of the particle in some medium.

3.2.1 UserAction methods

A useful feature of Geant4 is the ability to create user-defined actions (methods) throughout each module, which allows for a very fine-tuned analysis throughout the entire simulation. The following summarizes the custom details and methods for this application

- **DetectorConstruction.cc:** A copper cylinder of radius 3 cm and height 10 cm is covered in Kapton film of varying thickenesses: 59 μm, 100 μm and 200 μm. The film thickness is iterated by a function which is called before the command macro is examined. The top face of the copper lies in the $z = 0$ plane, with the beam approach the system from beneath.
- **SteppingAction.cc:** [For every step,] immediately checks if the step is the finale of a track. If so, the particle’s vertex (original position) and destination volume and coordinates are found, and a charge signal calculation occurs. Entering/Leaving the copper gives a net signal of $\pm q$

Table I. Geant4 Simulation Cylindrical Construction

Volume	Radius (mm)	Height (mm)
Copper	30	100
	Model	Thickness (μm)
Kapton1	S59	59
	S100	100
	S200	200
Silver	+Ag/KA	12
Kapton2	+Ag/KA	62

where q is the charge of the particle. Entering/Leaving Kapton gives a relative proportionality of

$$s_{q \rightleftharpoons KA} = \pm q \times \max\left[r_{\%}, z_{\%}\right], \tag{3}$$

where $r_{\%}$ is the percent distance away from the copper radially and $z_{\%}$ is the percent distance away laterally. The signals are grouped and saved by a unique eventID number.

- **EventAction.cc:** At the end of each event, the signals are tallied, grouped, and saved by a unique runID number.
- **RunAction.cc:** At the end of each run, the average and standard deviation of the signals are acquired.

3.2.2 Experimental parameters

Table I summarizes the detector geometry of each run. The order of logical volume layers starting from the innermost are 1) the copper cylinder, 2) the Kapton1 film, 3) the silver paint layer, and 4) the Kapton2 film. Constructing cylindrical “layers" is as straightforward as defining a cylinder within another’s logical volume. Data were acquired as a function of impinging proton energy using the 50-250 MeV range as used in the HIT experiment. The Kapton1 thickness optimization was applied to this model both with and without the silver and secondary Kapton (*+Ag/KA*).

4 RESULTS

(LATER: intro info here)

4.1 MCNP6 Simulation

Fig. 2 shows the variation of error with copper diameter and method. Two methods are compared, SRIM (reference) and MCNP6. A diameter of 6cm seems reasonable.

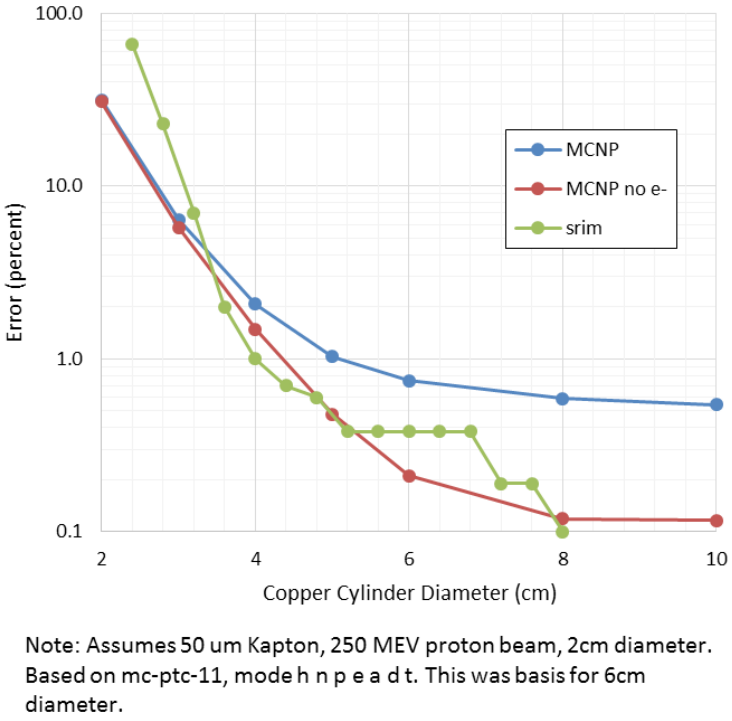

Figure 2. Signal Error vs Diameter and Simulation Method

The same calculation was repeated with proton tallies alone, i.e., without any secondary electrons. This shows that if electrons had been completely ignored, the MCNP6 results would have been similar to the SRIM model and a diameter of 8 cm would have seemed reasonable.

The distribution of proton collisions from 50 beam protons is in Fig. 3. The distribution of 6 other particles (born of 50 Protons) is in Fig. 4; neutrons go everywhere. The distribution of electrons (just type $SE_{!h}$) is similar to photons. Table II shows the boundary crossings of neutral particles. In the problem there are about two neutral particle boundary crossings per beam proton.

Table III shows the breakdown of gain from various charged particles for given directions and copper surfaces. This assumes 250 MeV Proton Beam, 6cm Copper Diameter and 50 microns kapton. The effect of secondary electrons produced directly by proton collisions (SD_h) is not included.

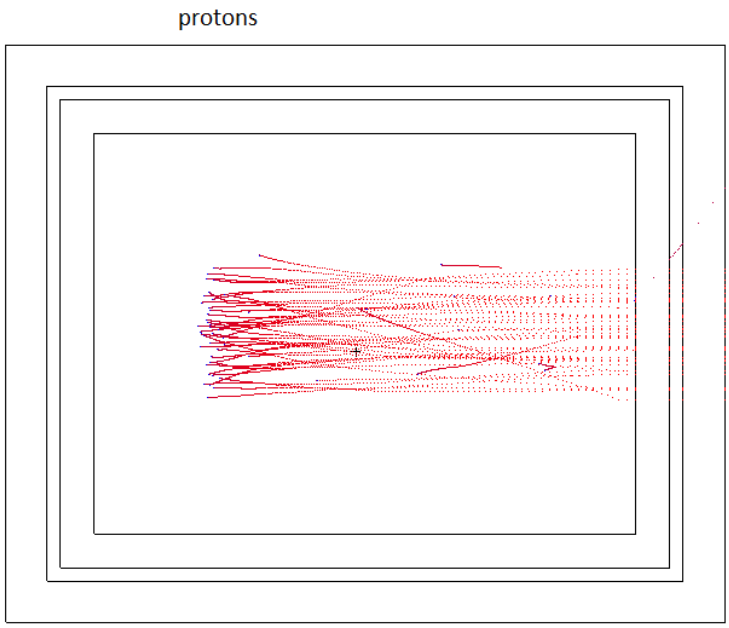

Figure 3. Distribution of 50 Protons of Energy 250 MeV using MCNP6. Note the singular backscatter.

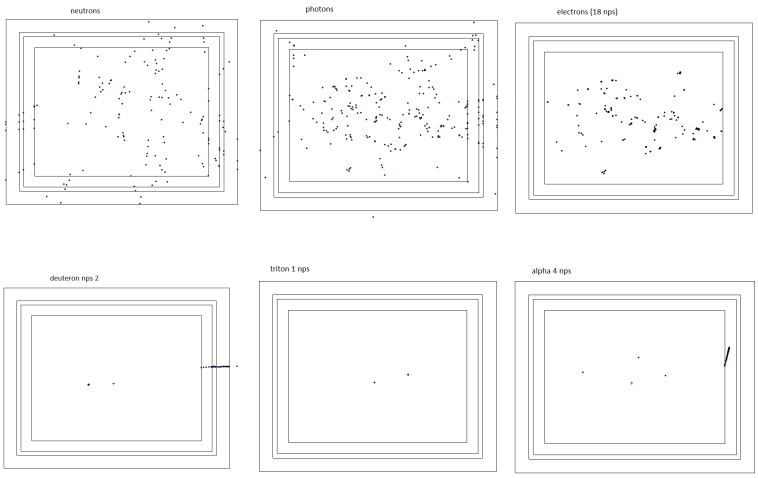

Figure 4. Distribution of six other particles

It is worth examining the behavior of the model. Kapton thickness (25, 50 and 75 microns) seems to make no difference in gain. Neither do the inclusion of tallies for deuterons, tritons and alphas, although the MCNP output file notes the absence of production cross-sections for these particles*. All of the figures and tables below were for the case of 6cm diameter, 50 microns of kapton and 50 beam protons of energy 250 MeV.

*The absence of ion production XS noted in the MCNP output file vs the presence of ions in the run needs to be checked out.

Table II. Charges Crossing Copper Surfaces (fraction per proton source) assuming 250 MeV Proton Beam, 6 cm Copper diameter, 50 microns of Kapton, and no SE_h

Particle	tally	face	cylinder	end	total
n	in	0.000 65	0.000 44	0.106 92	0.108 01
	out	0.148 74	0.678 67	0.000 07	0.827 47
γ	in	0.000 38	0.000 70	0.000 11	0.001 19
	out	0.176 03	0.650 51	0.078 12	0.904 66

Table III. Charges Crossing Copper Surfaces (fraction per proton source) assuming 250 MeV Proton Beam, 6 cm Copper diameter, 50 microns of Kapton, and no SE_h

Particle	tally	face	cylinder	end	total
P+	in	0.999 97	0.000 00	0.000 00	0.999 97
	out	0.000 55	0.001 23	0.000 23	0.002 01
	total	0.999 41	0.001 23	0.000 23	0.997 96
E (no SE_h)	in	0.000 31	0.000 87	0.000 10	0.001 28
	out	0.001 49	0.004 50	0.000 51	0.006 50
	total	0.001 19	0.003 62	0.000 42	0.005 23
d	in	0.000 03	0.000 00	0.000 00	0.000 03
	out	0.000 07	0.000 06	0.000 02	0.000 15
	total	0.000 04	0.000 06	0.000 02	0.000 12
t	in	0.000 02	0.000 00	0.000 00	0.000 02
	out	0.000 03	0.000 06	0.000 02	0.000 03
	total	0.000 01	0.000 06	0.000 02	0.000 01
a	in	0.000 03	0.000 00	0.000 00	0.000 03
	out	0.000 03	0.000 00	0.000 00	0.000 03
	total	0.000 00	0.000 00	0.000 00	0.000 00
Signal	in	0.999 74	0.000 87	0.000 10	1.001 24
	out	0.000 82	0.003 20	0.000 26	0.008 51
	total	0.998 23	0.004 85	0.000 65	0.992 73

4.2 Geant4 Simulation

The units of signal gain are $\frac{Q_{net}}{Q_P}$, where Q_{net} is the net transfer of charge into the cup, and Q_P is the net charge of the million protons irradiating the cup. Charges entering and leaving the primary Kapton film covering the copper are subject to the linear proportion behavior defined in Eq. 3. Table IV shows a sample output of each model in both air and vaccuum, the latter to remove oversaturation of beta emissions from the air due to delta-ray production (LATER: citation needed).

Table IV. Predicted Gain from High-Energy Protons using Geant4

Model	Energy (MeV)	(-Ag/KA)	(-Ag/KA) *in vacuo*	(+Ag/KA)	(+Ag/KA) *in vacuo*
S59	70.03	0.953 588	1.000 36	0.983 320	0.979 287
	100.46	0.967 417	1.000 68	0.982 263	0.979 775
	130.52	0.975 593	1.001 18	0.982 531	0.981 160
	160.09	0.981 094	1.001 77	0.983 127	0.982 672
	190.48	0.985 111	1.002 38	0.984 641	0.983 603
	221.06	0.988 151	1.003 14	0.986 131	0.985 152
	250.00	0.990 298	1.003 58	0.987 536	0.986 296
S100	70.03	0.953 827	1.000 36	0.983 731	0.979 531
	100.46	0.966 795	1.000 72	0.982 408	0.979 939
	130.52	0.975 725	1.001 21	0.982 508	0.980 993
	160.09	0.981 055	1.001 80	0.983 059	0.982 456
	190.48	0.985 189	1.002 45	0.984 910	0.983 649
	221.06	0.988 149	1.003 26	0.986 215	0.985 251
	250.00	0.990 324	1.003 49	0.987 278	0.986 103
S200	70.03	0.954 372	1.000 37	0.983 544	0.979 594
	100.46	0.966 915	1.000 68	0.982 554	0.979 769
	130.52	0.975 377	1.001 26	0.982 246	0.981 054
	160.09	0.980 998	1.001 78	0.983 405	0.982 137
	190.48	0.985 217	1.002 44	0.984 706	0.983 760
	221.06	0.988 312	1.003 20	0.986 402	0.984 905
	250.00	0.990 213	1.003 43	0.987 178	0.985 874

Fig. 5 depicts the tracks of particles given the simulation of 50 250 MeV protons entering the S59 model. The track color corresponds to particle charge, red for negative, blue for positive, and green neutral. As observed in the MCNP6 simulation, neutrons are scattered everywhere; for the most part, electrons created in the Faraday Cup do not travel far, as expected given their low-energy production and high stopping-power in copper.

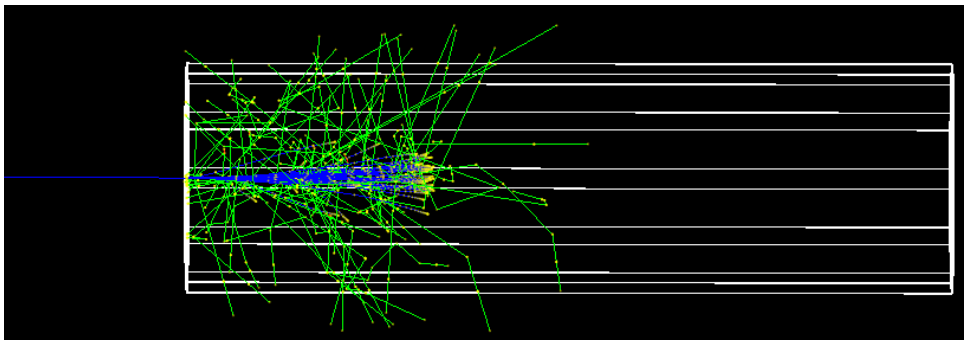

Figure 5. Distribution of 50 Protons of Energy 250 MeV using Geant4.

5 DISCUSSION

It is known that MCNP does not track electrons secondary to protons. Therefore, there are delta rays and secondary electrons from protons that have not been accounted for. This means that the error is greater than has been portrayed. This needs further investigation because it is shown in Fig. 2 that electrons (just the $SE_{!h}$) have an impact on the choice of diameter.

The electrons that are included are those that are secondary to the particle cascade subsequent to protons. For example, there are electrons secondary to photons that come from neutrons that come from protons. Table II shows that there are almost 2 neutral particles crossing the Faraday Cup boundary per beam proton.

It is important to note that the addition of deuterons, tritons and alphas changes the gain by -0.0002[†], and that there were no proton creation cross-sections for Ag-107, so it was substituted for Ag-109 which makes up about 2/3 of the silver.

In pursuit of the optimization of this portable Faraday Cup, we considered many variants of applicable theoretical models to corroborate with available experimental data. Fig. 6 depicts a very convincing similarity in behavior between the HIT beam stop measurements, and the simulation of the copper Faraday Cup in air without the *no* silver/Kapton layer.

6 CONCLUSIONS

7 ACKNOWLEDGMENTS

We would like to express our sincerest gratitude to Paul Romano and Tom Sutton, who provided the template for this paper.

[†]See mc-ptc-11-3.0-f for effect of deuterons, tritons, and alphas.

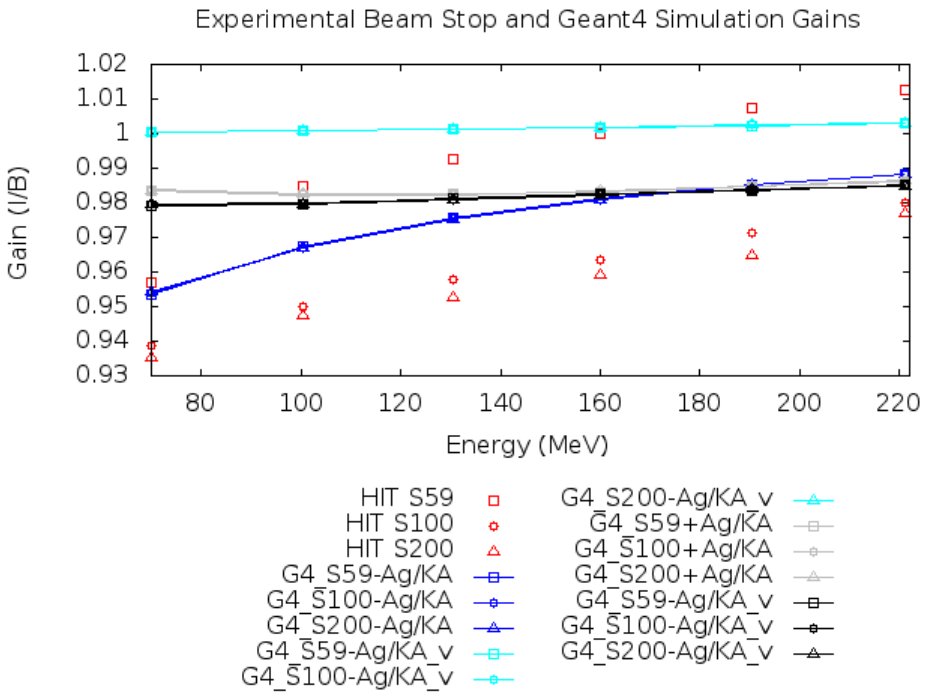

Figure 6. Comparison of Geant4 output and HIT measurement. Generated with Gnuplot.

8 REFERENCES

[1] J. Gordon and L. Magallanes, "Evaluation of Current Measuring Beam Stop," 2014, Proprietary Calculations.

APPENDIX A EXPERIMENTALS RESULTS AT HIT [1]

Table V. Measured Gain from HIT Beam Stops

Energy (MeV)	S59	S100	S200
70.03	0.9750	0.9385	0.9350
100.46	0.9850	0.9500	0.9475
130.52	0.9925	0.9580	0.9525
160.09	1.0000	0.9635	0.9590
190.48	1.0075	0.9715	0.9650
221.06	1.0125	0.9800	0.9770